NUMERICAL MODELING OF SPRAY COMBUSTION
WITH AN ADVANCED VOF METHOD

Yen-Sen Chen, Huan-Min Shang, Ming-Hsin Shih and Paul Liaw
Engineering Sciences, Inc.
Huntsville, AL 35802

ABSTRACT

This paper summarizes the technical development and validation of a multiphase computational fluid dynamics (CFD) numerical method using the volume-of-fluid (VOF) model and a Lagrangian tracking model which can be employed to analyze general multiphase flow problems with free surface mechanism. The gas-liquid interface mass, momentum and energy conservation relationships are modeled by continuum surface mechanisms. A new solution method is developed such that the present VOF model can be applied for all-speed flow regimes. The objectives of the present study are to develop and verify the fractional volume-of-fluid cell partitioning approach into a predictor-corrector algorithm and to demonstrate the effectiveness of the present approach by simulating benchmark problems including laminar impinging jets, shear coaxial jet atomization and shear coaxial spray combustion flows.

INTRODUCTION

The atomization, breakup and combustion processes of liquid propellant in many space transportation and propulsion systems are of vital importance to the combustion performance and stability of the system. Numerical modeling of these flows poses a challenge because it requires simultaneous resolution of liquid-gas-droplets dynamics, and the flow regimes considered can range from very low Mach number to high-speed compressible flows. The flow-process modeling is further complicated by surface tension, interfacial heat and mass transfer, material property variation, spray formation and turbulence, and their interactions. It is the aim of this study that a general and robust design analysis tool will be available as a result of the incorporation of advanced numerical and physical models in a computational fluid dynamics flow solver - FDNS code[1,2].

Conventionally, there have been some successful numerical algorithms for performing multiphase flow calculations involving free interfaces. In general, two basic approaches can be identified. One is based on the Lagrangian method and the other on the Eulerian frame work. The Lagrangian approach is to conform a mesh system with the sharp interface between gas and liquid and to track the movement of the interface according to sets of simplified equations governing the liquid and gas motions separately[3]. The entire Lagrangian grid network moves with the free surface which makes the grid generation or remeshing procedure very complex and CPU intensive. In the Eulerian approach, a fixed mesh system is used to resolve the sharp interface by the concept of a fractional volume of fluid (VOF)[4]. The second approach is more flexible and efficient in that it allows the resolution of the free surface to become part of the solution. The physical processes across the sharp interface such as surface tension forces, droplet or wave breakup, interphase mass transfer and condensation/vaporization, etc. can be modeled through the concept of a continuum surface force (CSF) method[5] or by the method of surface reconstruction as used in the ARICC3D code[6], SOLA-VOF code[4]. The CSF method is adopted in the present model for its generality and computational efficiency, especially for 3-dimensional computations.

Historically, developments of numerical methods for multiphase free surface flows were primarily aimed at incompressible flows utilizing the Volume of Fluid (VOF) method[7,8,9]. These methods are not effective for high-speed, high-Reynolds-number flows. So far, multiphase free surface flows have been considered in only a few general all-speed flow algorithms[6,10,11]. In the ARICC-3D Code[10], the VOF method was implemented in the ALE-ICE (Arbitrary Lagrangian Eulerian-Implicit Continuous-fluid Eulerian method) algorithm for injector flow simulation with atomization. Due to the inefficiency of the ALE-ICE method, the ARICC-3D was found very time-consuming for multi-element computations. The ALE-ICE was suggested to be replaced by a pressure-based SIMPLE algorithm[7] which may inprove the computational efficentcy. In the RIPPLE computer program[11],

only finite difference solutions to the incompressible Navier-Stokes equation are obtained on an Eulerian, rectangular mesh using a time-split two-step projection algorithm. Compressible fluids were not solved, while the surface tension is treated using the CSF method.

Based on a preliminary study of ref. 12, a unified multi-phase numerical method was developed. The gas-liquid interface mass, momentum and energy conservation properties are modeled by continuum surface mechanisms. A new solution method is developed such that the present VOF model can be applied for all-speed range flows. Numerical models for treating droplet dynamics are described in ref. 13. The main feature of the present method is to combine the advanced interface models of the Volume of Fluid (VOF) method and the Eulerian/Lagrangian method used in a pressure-based particulate two-phase flow solver[1, 2, 13] into a unified algorithm for efficient non-iterative, time-accurate calculations of multiphase free surface flows valid at all speeds. The present method reformulates the VOF equation to strongly couple two distinct phases (liquid and gas), and tracks droplets on a Lagrangian frame when a spray model is required, using a unified predictor-corrector technique to account for the non-linear linkages through the convective contributions of the VOF function. The CSF model is employed to model the surface tension forces. Formations of droplets and tracking of droplet dynamics are handled through the same predictor-corrector solution procedure. Thus the new algorithm is non-iterative and is flexible in the handling of any general geometries with arbitrarily complex topology in free surfaces. The present method can be applied for transient and steady state computations and can be implemented into any pressure-based solution method.

GOVERNING EQUATION

VOF methods have been mainly developed and used for low-speed flows such that incompressibility can be assumed. The incompressible flow assumption limits their capability. To generalize, the present formulation is based on compressible flow governing equations. The forms of the equations are then continuously reduced to their incompressible forms according to the local flow conditions and the VOF solutions. This is the uniqueness of the present method. To illustrate this, the density-weighted averaged conservation equation of mass, Navier-Stokes, and scalar variables in an Eulerian frame work can be written as:

$$\frac{\partial \rho_m}{\partial t} + \frac{\partial \rho_m u_j}{\partial x_j} = S_m$$

$$\frac{\partial \rho_m u_i}{\partial t} + \frac{\partial \rho_m u_j u_i}{\partial x_j} = -\frac{\partial p}{\partial x_i} - \frac{\partial}{\partial x_j}\left(\overline{\rho u'_i u'_j}\right) + D_a + S_a \qquad (1)$$

$$\frac{\partial \rho_m \phi}{\partial t} + \frac{\partial \rho_m u_j \phi}{\partial x_j} = -\frac{\partial}{\partial x_j}\left(\overline{\rho u'_j \phi'}\right) + D_\phi + S_\phi$$

where D and S represent diffusion and source terms respectively. The VOF transport equation is given below.

$$\frac{\partial \alpha}{\partial t} + u_i \frac{\partial \alpha}{\partial x_i} = S_\alpha \qquad (2)$$

where $\alpha = 1$ stands for liquid and $\alpha = 0$ is for gas. The interface is located at $1 > \alpha > 0$. S_α represents the volume transfer rate across the two-phase boundaries. And, $\rho_m = (1-\alpha)\rho_g + \alpha\rho_l$ where ρ_m denotes the time-mean density of the mixture, ρ_g and ρ_l denote gas and liquid density respectively, u_i and u'_i are the i-component of the density-weighted mean and fluctuating part of the instantaneous velocity, ϕ and ϕ' are the density-weighted mean and fluctuating part of the instantaneous scalar quantities including the species concentrations, turbulence quantities and the gas mixture enthalpy, p is the mean pressure and S is used to model sources terms due to mass transfer, momentum transfer, species production, etc. The mixture density is used in the governing equation to represent the present continuum interface model. For pure-liquid or pure-gas regions, the density would recover liquid density or gas density respectively based on the mixture density and the interface definitions. Detailed

expressions of the source terms can be found in refs. 1 and 2. In the present study, the turbulence correlation terms, $\overline{u'_i u'_j}$ and $\overline{u'_i \phi'}$, are modeled by the two-equation turbulence closure models[14] using eddy viscosity formulations. For a given solution of the α field, equation (1) can be rewritten as the following form to maintain accurate transient from the gas-phase flowfield to the liquid-phase flowfield through the interface.

$$\frac{\partial \rho_m \phi}{\partial t} + \frac{\partial \rho_m u_i \phi}{\partial x_i} = S_\phi, \quad \alpha < 0.01 \qquad \text{for compressible gas}$$

$$\rho_m \frac{\partial \phi}{\partial t} + \rho_m u_i \frac{\partial \phi}{\partial x_i} = S_\phi, \quad \alpha \geq 0.01 \qquad \text{for interface and liquid}$$

CONTINUUM SURFACE TENSION FORCE MODEL

The surface tension forces in the continuum surface force (CSF) model are formulated as continuous body forces across the interface. These forces can be written as,

$$F_x = -\sigma \left(\nabla \cdot \hat{n} \right) \alpha_x$$

$$F_y = -\sigma \left(\nabla \cdot \hat{n} \right) \alpha_y + \left(\frac{|\alpha_y|}{y} \right) \Big/ \text{for 2D axisymetric only}$$

$$F_z = -\sigma \left(\nabla \cdot \hat{n} \right) \alpha_z, \quad \text{---for 3D case only}$$

where σ denotes the surface tension coefficient and $\hat{n}$ stands for a unit normal vector at the interface calculated based on the solution of α.

INTERFACE MASS TRANSFER MODEL

To simulate the mass transfer effects along the interface of the gas and liquid phases, the source term of Eq. (2) is modeled. The sign and magnitude of the VOF source term, S_α in Eq. (2), depend on the physical processes involved. For spray atomization applications, for instance, it would represent the volume stripping rate which can be modeled by atomization correlations. For spray coating, condensation and chemical vapor deposition processes, on the other hand, positive volume flow rates would result.

There are basically two ways of modeling the VOF source term. One method is to treat the inter-phase volume flow rate as convection process along the interface. That is,

$$S_\alpha = V_s \cdot \nabla \alpha$$

where V_s denotes the volume exchange velocity. This method allows the source term and the convection terms be combined so that the source effects are handled implicitly. However, the accuracy of this approach depends entirely on the assignment of the volume exchange velocity. Vectors directly normal to the interface do not always guarantee good solution.

The second approach, which is the most straight forward treatment, solve the VOF equation with the source term specified explicitly. This approach is general and provides good numerical accuracy. The only drawback of this method is the possible numerical instability related to high volume flow rates. Time step size must be small enough in order to solve the VOF equation with large source term. For shear coaxial spray, empirical correlations such as the Reitz model[15] can be used to calculate the mass stripping rate and spray atomization droplet size distributions. In order to provide better interfacial resolution which is essential for the success of the present VOF method, all test cases were simulated with a high-order upwind Total Variation Diminishing (TVD)

Scheme. Only the convection terms were modeled by using the TVD flux limiters. The convection terms of the VOF transport equation can be expressed by finite difference approximation as:

$$\frac{\partial F}{\partial \xi} = f_{i+1/2} - f_{i-1/2} + h_{i+1/2} - h_{i-1/2}$$

where f and h represent first-order fluxes and TVD flux limiters respectively. The TVD flux limiters function as anti-diffusion terms to recover high-order accuracy. The first-order fluxes and the TVD flux limiters are given below.

$$f_{i+1/2} = \max\{0,(\rho U)_{i+1/2}\}\phi_i + \max\{0,-(\rho U)_{i+1/2}\}\phi_{i+1}$$

$$h_{i+1/2} = \begin{cases} \frac{1}{4}|\rho U|_{i+1/2}\{d\phi^+_{i+1/2} + d\phi^-_{i-1/2} + \gamma(d\phi^+_{i+1/2} - d\phi^-_{i-1/2})\}, U \geq 0 \\ \frac{1}{4}|\rho U|_{i+1/2}\{d\phi^-_{i+1/2} + d\phi^+_{i+3/2} + \gamma(d\phi^-_{i+1/2} - d\phi^+_{i+3/2})\}, U < 0 \end{cases}$$

where the minmod functions in the TVD flux limiters are written as:

$$d\phi^{\pm}_{i+1/2} = \text{sign}(\Delta\phi_{i+1/2})\max\left\{0, \min\left[|\Delta\phi_{i+1/2}|, \beta\,\text{sign}(\Delta\phi_{i+1/2})\Delta\phi_{i-(-1/2\pm1)}\right]\right\}$$

The order of accuracy of this scheme is determined by the parameters γ and β. Only the second-order upwind schemes was used in this study. That is,

$$\beta = \text{Compression} - \text{Factor} = \frac{3-\gamma}{1-\gamma}$$

where $\gamma = -1$. The compression factor, β, is used to sharpen the interface for better resolution.

COMBUSTION MODEL

For reacting flow computations, a penalty function treatment[16, 17] of the reacting source terms is employed to calculate the source terms of the species equaitons. Finite-rate chemical kinetics for the O2/H2[18] and O2/RP-1/H2[19] systems were employed for good representation of the reacting flow development. Global reaction models were used during the ignition and flame spreading period to achieve better computational efficiency for spray combustion applicaitons. This approach is justified for steady-state calculations.

VALIDATION

LAMINAR IMPINGING JETS

Impinging elements are common in injector designs. The prediction of the liquid sheet development has been a challenging task for most CFD methods. With the present VOF model, the problem of modeling the liquid jets impingement process is solved with very minimal computational effort. In this test case, three impinging water jets with different impinging half angle (i.e. 30°, 45° and 60°) were considered. A grid size of 61 x 41 x 41 was generated to simulate the three-dimensional flowfields. The injection speed was 10 m/s and the flowfields were assumed to be laminar. The calculation, which was a transient approach, was terminated at 200 time steps before sheet breakup may occur. Figure 1 shows the predicted flowfields and liquid surface shapes for the three jets. A thin sheet of liquid was formed after impingement. Figure 2 shows the liquid sheet thickness distribution function and comparisons with an exact solution given by ref. 20. Good agreement is revealed in the data comparisons. Future development effort shall include models for atomization and turbulence effects on jet impingement.

SHEAR COAXIAL LIQUID JET ATOMIZATION

A cold flow case of coaxial liquid jet atomization reported by Pal, et al[21] was employed to test the current numerical method. Water and gaseous nitrogen were used as the liquid and gas in the study with injection velocity 14.3 m/s and 293 m/s (Mach number around 0.86) respectively. The operating conditions were 300-k temperature and one atmospheric pressure. A grid size of 61 x 31 was used for the computation. Droplet evaporation effects were considered, which is not important in this case. Figure 3 shows the velocity vectors and liquid core. Liquid jet velocity stays fairly constant due to large density difference between two fluids. The numerical model is stable even for large time-step size and incompressible (liquid) /compressible (gas) flow situation. Figure 4 presents the particle size variations and locations. Particle turbulent dispersion effect has been included and large particle dispersion is shown due to high turbulent intensity of the gas phase. The numerical prediction is reasonable compared to the observed main flow feature[21].

SHEAR COAXIAL INJECTOR SPRAY COMBUSTION

A test case of LOX/H2 coaxial spray with the same operating conditions as the Case D of the Penn State uni-element experiment was investigated with the present VOF/particulate multi-phase model and a 7-step H2/O2 finite rate chemical kinetics. The LOX and GH2 flowrates were 0.373 lbm/sec and 0.072 lbm/sec respectively. The velocity ratio at the injector outlet was 28.6 with the hydrogen gas going at a relatively high speed around Mach 0.6. The mean droplet size of the primary atomization under the operating conditions was about 30 micron. A mesh with size 121 x 61 was used for the computation. A cold flow case was calculated for 1000 time steps to have a better gas mixture established before a hot spot of 1000 degree-K was introduced near the chamber wall in the middle of the chamber length. Once the flame was started it spread in both upstream and downstream directions. At the final stage the flame front was going very slowly upstream until it's near the injector face. The total number of time steps for one case was around 5000 (nondimensional time step size of 0.2). Results of the computations are shown in Figure 5 for the temperature and particle fields. These results give reasonable representation of the observed experimental flowfield. The liquid jet interface is also shown in Figure 5b. The calculated chamber pressure is a little higher (10 percent) than the measured value indicating larger flame zone was predicted. This is relating to the turbulence mixing problem.

Another case for LOX/RP-1/H2 tripropellant coaxial injector case is also investigated. Same chamber geometry as the previous case, except for the injector details which was designed by the author, was used. The LOX, RP-1 and H2 flowrates were assumed to be 0.9659 lbm/sec, 0.1393 lbm/sec and 0.0495 lbm/sec respectively. This high flow rates produced a high chamber pressure around 38 ATM. As opposed to the LOX/H2 case, the ignition process for this case was some what tricky. A flame zone was finally established after many attempts of igniting the propellant. More investigation is needed to study the key factor affecting the ignition process. Preliminary results of this case are shown in Figure 6. It is clear that a much longer stand-off distance was predicted for this case. The particle and VOF surface plot (Figure 6b) shows that the current multiple VOF model is working.

CONCLUSIONS

This paper summarizes the technical development and validation of a unified multiphase computational fluid dynamics (CFD) numerical method using volume-of-fluid (VOF) model which can be employed to analyze general multiphase flow problems involving free surface. A time-accurate multiphase viscous flow solution method has been developed and validated with benchmark test cases including laminar impinging jets and a coaxial jet spray atomization simulation. The gas-liquid interface mass, momentum and energy conservation properties are modeled by continuum surface force mechanisms. A new solution method is developed such that the present VOF model can be applied for all-speed flow regimes. The main achievements of the present study are the development and verification of the fractional volume-of-fluid cell partitioning approach into a predictor-corrector algorithm to deal with multiphase (gas-liquid) free surface flow problems; and the coupling of this unified all-speed algorithm with a non-iterative Eulerian/Lagrangian particle tracking and finite-rate chemistry model. The successful implementation of the VOF model in this study can lead a reliable numerical model for

spray atomization and combustion flow analyses as well as a fundamental building block for a numerical tool which can be used to study complex multiphase flow phenomena which are sometimes hard to visualize experimentally.

REFERENCES

1. Wang, T. S. and Chen, Y. S., "Unified Navier-Stokes Flowfield and Performance Analysis of Liquid Rocket Engines," *J. Propulsion and Power*, Vol. 9, No. 5, pp. 678-685, 1993.
2. Chen, Y. S., Liaw, P., Shang, H. M., and Chen, C. P., "Numerical Analysis of Complex Internal and External Viscous Flows with a Second-Order Pressure-Based Method," AIAA Paper No. 93-2966, 1993.
3. Harlow, F. H. and Welch J. F., " Numerical Calculation of Time-Dependent Viscous Incompressible Flow with Free Surface," *Phys. Fluids*, Vol. 8, p. 2182, 1965.
4. Hirt, C. W. and Nichols, B. D., "Volume of Fluid (VOF) Method for the Dynamics of Free Boundaries," *J. of Comp. Phys.*, Vol. 39, p. 201, 1981.
5. Brackbill, J. U., Kothe, D. B. and Zemach, C., "A Continuum Method for Modeling Surface Tension," *J. Comp. Phys.*, Vol. 100, p.335, 1992.
6. Liang, P. and Chan, D. C., "Development of A Robust Pressure - Based Numerical Scheme for Spray Combustion Applications," AIAA Paper No. 93-0902, 1993.
7. Nichols, B. D., Hirt, C. W. and Hotchkiss, R. S., "SOLA-VOF: A Solution Algorithm for Transient Fluid Flow with Multiple Free Boundaries," Los Alamos, LA-8355, 1980.
8. Torrey, M. D., Cloutman, L. D., Mjolsness, R. C. and Hirt, C. W., "NASA - VOF2D; A Computer Program for Incompressible Flows with Free Surfaces," LA-10612-MS, Los Alamos National Lab, 1985.
9. Liu Jun, "Computer Modeling of Flows with a Free Surface," Ph. D. Thesis, Imperial College, London, 1987.
10. Liang, P. and Ungewitter, R., "Multi-phase Simulations of Coaxial Injector Combustion," AIAA Paper No. 92-0345, 1992.
11. Kothe, D. B. and Mjolsness, R. C., "RIPPLE: A New Model for Incompressible Flows with Free Surfaces," *AIAA J.* Vol. 30, p. 2694, 1992.
12. Seung, S. P., Chen, Z. J., Chen, C. P., Chen, Y. S. and Wang, T. S., "A Combined Eulerian-VOF-Lagrangian Method for Atomization Simulations," 30th JANNAF Combustion Subcommittee Meeting, 1993.
13. Chen, C. P., Shang, H. M. and Jiang, "An Efficient Pressure-Velocity Procedure for Gas-Droplet Two-Phase Flow Calculations," *Int. J. Numer. Method Fluid*, Vol. 15, p.233, 1992.
14. Chen, Y. S. and Kim, S. W., "Computation of Turbulent Flows Using an Extended k-ε Turbulence Closure Model," NASA CR-179204 1987.
15. Reitz, R.D., "Modeling Atomization Processes in High-Pressure Vaporizing Sprays," *Atomization and Spray Technology*, Vol. 3, pp.309-337, 1987.
16. Chen, Y.S. and Farmer, R.C., "Computations of Premixed and Diffusion Flames with a Fast Chemistry Integration Scheme," 4th ISCFD, U.C. Davis, pp. 172-177, 1991.
17. Wang, T.S., McConnaughey, P., Warsi, S. and Chen, Y.S., "CFD Assessment of the Pollutant Environment from RD-170 Propulsion System Testing," AIAA Paper 95-0811, 33rd Aerospace Sciences Meeting, 1995.
18. Jachimowski, C.J., "An Analytical Study of the Hydrogen-Air Reaction Mechanism with Application to Scramjet Combustion," NASA TP 2791, 1988.
19. Wang, T.S., "Thermo-Kinetics Characterization of Kerosene/RP-1 Combustion for Tri-Propellant Engine Design Calculations," JANNAF Meeting, 7th Annual Symposium, Marshall Space Flight Center, 1995.
20. Hasson, D. and Peck, R.E., "Thickness Distribution in a Sheet Formed by Impinging Jets," A.I.Ch.E. Journal, Vol. 10, No. 5, pp. 752-754, 1964.
21. Pal, S., Moser, M.D., Ryan, H.M., Foust, M.J. and Santoro, R.J., "Flowfield Characteristics in a Liquid Propellant Rocket," AIAA Paper 93-1882, 1993.
22. Beisler, M.A., Pal, S., Moser, M.D., and Santoro, R.J., "Shear Coaxial Injector Atomization in a LOX/GH2 Propellant Rocket," AIAA 94-2775, 30th AIAA/ASME/SAE/ASEE Joint Propulsion Conference, June 27-29, 1994.
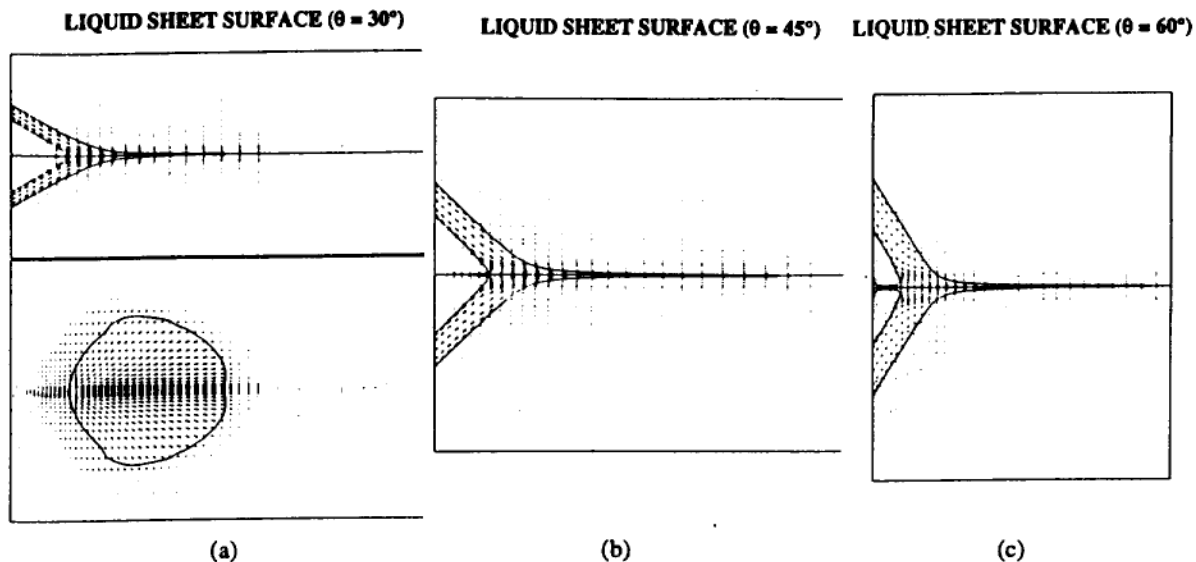
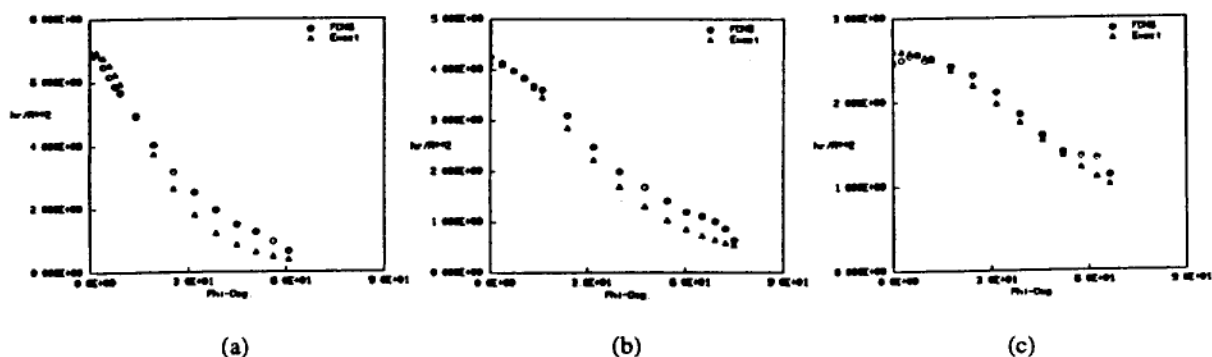**Figure 1.** Laminar impinging jet flowfield. Impinging angle: (a) 30°; (b) 45° and (c) 60°.

Figure 2. Liquid sheet thickness distributions and data comparisons. Impinging angle: (a) 30°; (b) 45° and (c) 60°.
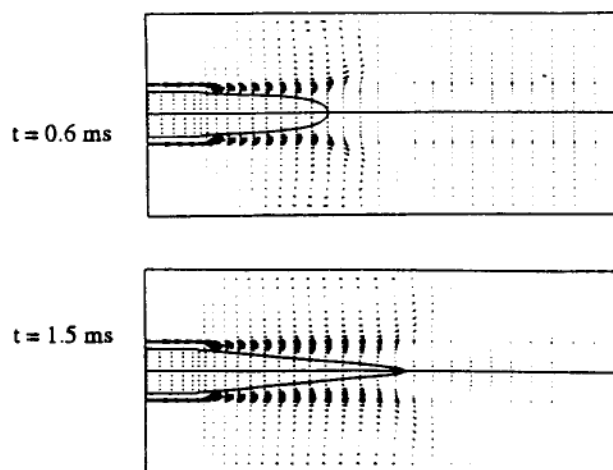

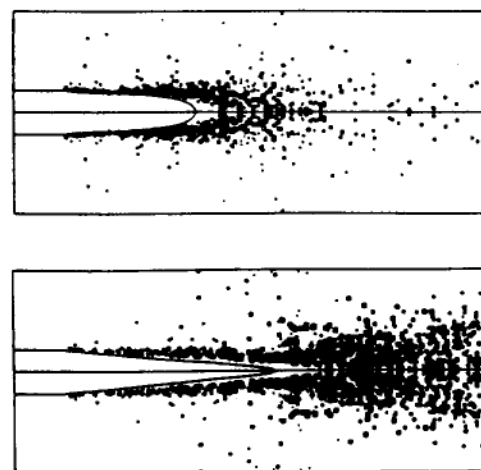**Figure 3.** Velocity vector and liquid core.

Figure 4. Particle trajectories.